Inorganic Chemistry

Article

pubs.acs.org/IC

Synthesis, Structures, and Magnetic Properties of End-to-End Azide-Bridged Manganese(III) Chains: Elucidation of Direct Magnetostructural Correlation

Jeong Hwa Song,[†] Kwang Soo Lim,[†] Dae Won Ryu,[†] Sung Won Yoon,[‡] Byoung Jin Suh,[‡] and Chang Seop Hong*,[†]

[†]Department of Chemistry, Research Institute for Natural Sciences, Korea University, Seoul 136-713, Korea

[‡]Department of Physics, The Catholic University of Korea, Buchon 420-743, Korea

Supporting Information

ABSTRACT: The two one-dimensional chain compounds $[Mn(\mathbf{L1})(N_3)]\cdot H_2O$ ($\mathbf{1}\cdot H_2O$; $H_2\mathbf{L1}$ = 2,2′-((1*E*,1′*E*)-ethane-1,2-diylbis(azan-1-yl-1-ylidene))bis-(phenylmethan-1-yl-1-ylidene)diphenol) and $[Mn(\mathbf{L2})(N_3)]$ (**2**; $H_2\mathbf{L2}$ = 2,2′-((1*E*,1′*E*)-2,2-dimethylpropane-1,3-diyl)bis(azan-1-yl-1-ylidene)-bis(phenylmethan-1-yl-1-ylidene)diphenol) bridged by single end-to-end azides were prepared via a self-assembly process. Each Mn(III) ion exhibits a characteristic Jahn−Teller elongation along the chain direction. For both compounds, antiferromagnetic interactions between Mn(III) spins within a chain are transmitted through the azide ligands, together with the apparent occurrence of spin canting at low temperatures. Remarkably, the coupling constants (*J*) for **1** and **2** exceed those reported for end-to-end azide-linked Mn(III) systems. A systematic magnetostructural relationship based on the torsion angle is established in terms of the torsion angle $Mn-N_{ax}\cdots N_{ax}-Mn$ (ax = axial) for the first time.

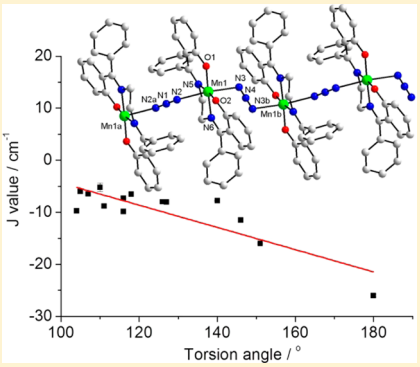

INTRODUCTION

The construction of molecular magnetic entities with fascinating characteristics requires a judicious selection of spin carriers and bridging groups as efficient magnetic couplers. Examples of promising linkers include oxides, cyanides, carboxylates, and azides that have short magnetic paths for effective superexchange coupling.[1] Azide has been intensely explored to attain coordination systems from zero-dimensional to three-dimensional structures.[2−12] Structural diversity is derived from the various binding modes of azide, including end-on (EO) and end-to-end (EE).[13] Another recognized feature of the azide ligand is the predictability of the magnetic coupling: azide in the EO mode mediates ferromagnetic interactions and azide in EE communicates antiferromagnetic coupling with some exceptional examples.[14−16]

On the basis of the versatile binding conformations of the azide ligand, a rich family of coordination complexes employing 3d paramagnetic metal ions has been unearthed. When magnetic anisotropy is incorporated into a lattice, magnetic features such as single-molecule magnet and single-chain magnet properties, canting behavior, and long-range magnetic order emerge.[9,11,17−21] In particular, the high-spin Mn(III) ion stabilized by the N_2O_2 donors of a tetradentate Schiff base has been found to offer significant uniaxial anisotropy associated with the Jahn−Teller elongation.[22] The cationic Mn(III) Schiff bases have two axial positions available for incoming ligands. These coordination sites can accommodate azide anions to form mononuclear or one-dimensional (1D) chain structures. In the case of the 1D systems, the azide ligand can singly bridge neighboring Mn(III) ions in the EO or EE mode. The 1D series displayed the anisotropy-related properties of the spin-canting phenomenon, slow magnetic relaxation, field-induced phase transition, and long-range order.[23−32] The singly azide bridged systems offer a platform for a straightforward understanding of the coupling nature and strength, contingent on the metric parameters of the single exchange pathway. In the analysis of the coupling constant (*J*) of select complexes with a single EE bridge, the largest *J* value obtained was $-11.5\ cm^{-1}$ for an azide-linked Mn(III) Schiff base chain.[32] Various attempts have been made to account for the magnetic coupling nature in view of the structural parameters such as bond length, bond angle, and torsion angle in the bridging route.[28,32,33] However, a systematic magnetostructural correlation was not established for such systems, although it is of utmost importance to achieve in-depth insight into the magnetic mechanism of molecule-based magnetic systems.

Herein we report the synthesis, structures, and properties of the 1D coordination polymers $[Mn(\mathbf{L1})(N_3)]\cdot H_2O$ ($\mathbf{1}\cdot H_2O$) and $[Mn(\mathbf{L2})(N_3)]$ (**2**). Chemical structures of the Schiff base ligands used in the synthesis of **1** and **2** are given in Scheme 1. Both complexes show intrachain antiferromagnetic interactions and record-high exchange coupling constants among single EE azide-based Mn(III) systems. The magnitude of the magnetic

Received: March 23, 2014
Published: July 18, 2014

   dx.doi.org/10.1021/ic500676k | *Inorg. Chem.* 2014, 53, 7936−7940

Scheme 1. Chemical Structures of the Schiff Base Lignads Used in the Synthesis of 1 and 2

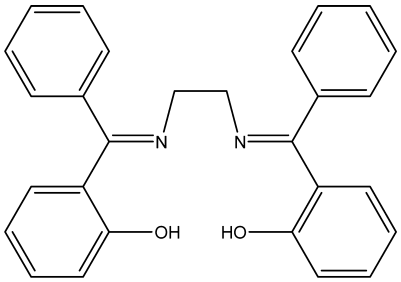

H_2L1: 2,2'-(1*E*,1'*E*)-(ethane-1,2-diylbis(azan-1-yl-1-ylidene))-bis(phenylmethan-1-yl-1-ylidene)diphenol

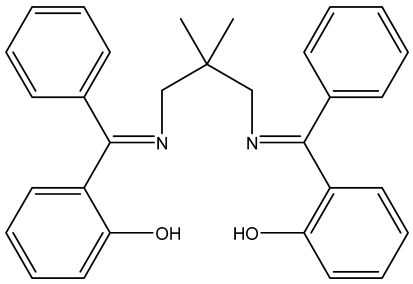

H_2L2: 2,2'-(1*E*,1'*E*)-(2,2-dimethylpropane-1,3-diyl)bis(azan-1-yl-1-ylidene)-bis(phenylmethan-1-yl-1-ylidene)diphenol

interactions is correlated with the variation of the torsion angle, as revealed for the first time.

EXPERIMENTAL SECTION

General Procedures and Materials. All chemicals and solvents used for synthesis were of reagent grade and were used as received. Mn Schiff bases were synthesized according to modified literature methods.[34,35]

[Mn(L1)(N_3)]·H_2O (1·H_2O). At room temperature, solid NaN_3 (32.5 mg, 0.5 mmol) was added to a stirred methanol solution (100 mL) of Mn(**L1**)ClO_4 (295.5 mg, 0.5 mmol). After it was stirred for several minutes, the mixture was refluxed for 12 h. Brown crystals were obtained from solution by slow evaporation. The crystals were filtered off, washed with methanol, and dried in air. Yield: 20.4% (52.8 mg). Anal. Calcd for $C_{28}H_{22}MnN_5O_2$: C, 63.04; H, 4.53; N, 13.13. Found: C, 63.20; H, 4.13; N, 12.90. The IR spectrum is reported in Figure S1 (Supporting Information).

[Mn(L2)(N_3)] (2). The preparation of **2** was similar to that described for **1**, except that Mn(**L2**)ClO_4 (0.2 mmol) in methanol was used instead of Mn(**L1**)ClO_4. Dark brown platelike crystals were obtained by slow evaporation. Yield: 10.3% (20.6 mg). Anal. Calcd for $C_{93}H_{84}Mn_3N_{15}O_6$: C, 66.78; H, 5.06; N, 12.56. Found: C, 66.79; H, 4.95; N, 12.54. The IR spectrum is reported in Figure S1 (Supporting Information).

Physical Measurements. Elemental analyses for C, H, and N were performed at the Elemental Analysis Service Center of Sogang University. Infrared spectra were obtained from KBr pellets with a Nicolet-380 spectrometer (Thermo Electron Corp.). Magnetic susceptibilities for **1** (12.6 mg) and **2** (10 mg) were carried out using a Quantum Design SQUID susceptometer (dc) and a PPMS magnetometer (ac). The diamagnetic corrections of **1** and **2** were estimated from Pascal's tables.

Crystallographic Structure Determination. X-ray data for **1** and **2** were collected on a Bruker SMART APEXII diffractometer equipped with graphite-monochromated Mo Kα radiation (λ = 0.71073 Å). Preliminary orientation matrix and cell parameters were determined from three sets of ϕ (**1**) and ω (**2**) scans at different starting angles. Data frames were obtained at scan intervals of 0.5° with an exposure time of 10 s (**1**) and 30 s (**2**) per frame. The reflection data were corrected for Lorentz and polarization factors. Absorption corrections were carried out using SADABS. The structures of **1** and **2** were solved by direct methods and refined by full-matrix least-squares analysis using anisotropic thermal parameters for non-hydrogen atoms with the SHELXTL program. All hydrogen atoms were calculated at idealized positions and refined with the riding models. Crystal data of **1**: M_r = 515.45, monoclinic, space group $P2_1/n$, a = 10.1192(13) Å, b = 23.290(3) Å, c = 11.2686(14) Å, β = 113.551(6)°, V = 2434.5(6) Å^3, Z = 4, D_{calcd} = 1.406 g cm^{-3}, μ = 0.578 mm^{-1}, 17010 reflections collected, 5523 unique (R_{int} = 0.0477), R1 = 0.0473, wR2 = 0.0876 ($I > 2\sigma(I)$). Crystal data of **2**: M_r = 1672.57, orthorhombic, space group $P2_12_12_1$, a = 13.4912(3) Å, b = 18.9024(5) Å, c = 32.0832(7) Å, V = 7926.7(3) Å^3, Z = 4, D_{calcd} = 1.402 g cm^{-3}, μ = 0.538 mm^{-1}, 41649 reflections collected, 18958 unique (R_{int} = 0.0531), R1 = 0.0621, wR2 = 0.1321 ($I > 2\sigma(I)$).

RESULTS AND DISCUSSION

Description of the Structures. The structures of **1** and **2** have been characterized using single-crystal X-ray diffraction techniques. The use of Mn(III) Schiff bases with different linkers affords the monoclinic crystal system ($P2_1/n$) for **1** and orthorhombic crystal system ($P2_12_12_1$) for **2**. The crystal structures of **1** and **2** are depicted in Figure 1. Each Mn atom

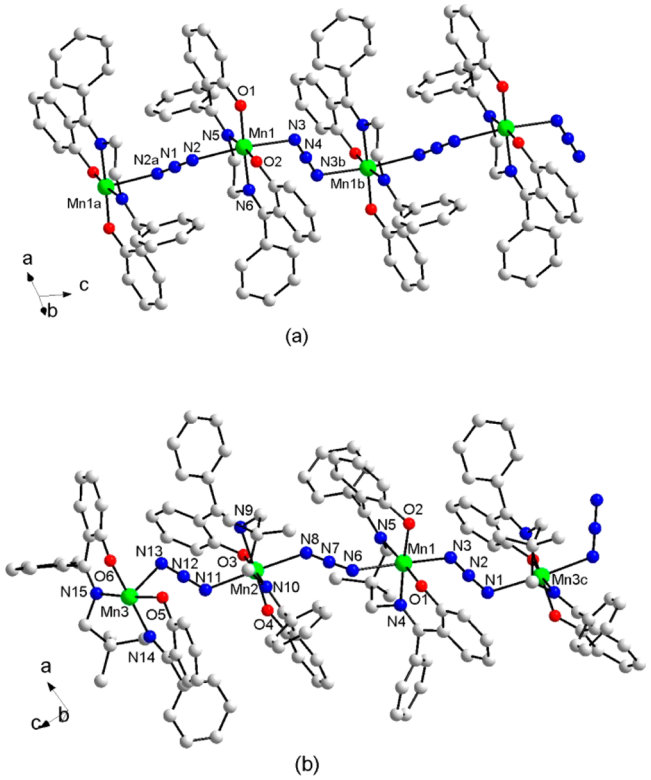

Figure 1. Molecular views of (a) **1** and (b) **2** with the atom-labeling schemes. Symmetry codes: (a) 1 − x, 2 − y, 1 − z; (b) 1 − x, 2 − y, 2 − z; (c) 1.5 − x, 1 − y, −0.5 + z.

occupies the central position of an octahedral environment consisting of the N_2O_2 donors from **L1** and two N atoms from the azides. For **1**, the typical Jahn−Teller elongation is present in each Mn(III) ion, as judged by the short equatorial (eq) Mn−N(O)$_{eq}$ bond lengths (average Mn−N(O)$_{eq}$ = 1.93(8) Å) and the long axial (ax) Mn−N_{ax} distances (Mn1−N2 =

dx.doi.org/10.1021/ic500676k | Inorg. Chem. 2014, 53, 7936−7940

2.279(2) Å, Mn1−N3 = 2.286(2) Å).[22−31] The Mn−N−N bridging angles are 121.39(13)° for Mn1−N2−N1 and 119.72(14)° for Mn1−N3−N4, and the torsion angle Mn−N_{ax}···N_{ax}−Mn corresponds to 180°, which marks the largest value among EE azide-bridged Mn(III) systems.[23,27,28,32,33,36,37]

The azide ligands bridge the Mn centers in an EE mode to form a 1D chain structure running along the *c* axis (Figure S2, Supporting Information). The Mn1−Mn1a intrachain distance (symmetry code: (a) $1 - x, 2 - y, 1 - z$) is 6.086(1) Å, and the shortest interchain Mn−Mn separation is 7.315 Å. In the case of **2**, similar structural features are present, although there are three crystallographically distinct Mn(III) sites in the structure. Each Mn ion is subject to the Jahn−Teller distortion; the short Mn−$N(O)_{eq}$ distance is 1.96(8) Å, whereas the long apical Mn−N_{ax} lengths range from 2.244(3) to 2.314(3) Å. The Mn−N−N angles in the bridging skeleton span the range of 114.6(3) to 134.9(3)°, and the torsion angles of Mn−N_{ax}···N_{ax}-Mn range from 143.8(2) to 154.3(2)°. Within a chain, the intrachain Mn−Mn distances are 6.1251(1) Å for Mn1−Mn2, 6.1588(1) Å for Mn1−Mn3c (symmetery code: (c) $1.5 - x, 1 - y, -0.5 + z$), and 5.9208(1) Å for Mn2−Mn3. The chain runs along the *c* direction in a zigzag pattern, and the shortest distance between Mn atoms is 9.909 Å (Figure S3, Supporting Information).

Magnetic Properties. The temperature dependence of the magnetic susceptibilities for **1** and **2** was measured at $H = 1$ kG and $T = 2$−300 K (Figure 2). At 300 K, the $\chi_m T$ values of **1** and **2** were equal to 1.83 and 2.27 cm^3 K mol^{-1}, respectively, which are lower than that (3.00 cm^3 K mol^{-1}) anticipated for an isolated high-spin Mn(III) ($S_{Mn} = 2$) ion. As the temperature decreased, $\chi_m T$ underwent a slow reduction and an anomaly was apparent at low temperature. The gradual decline in the curve indicates the operation of antiferromagnetic interactions between spin centers. A low-*T* hump was clearly visible in the $\chi_m T$ plot when lower magnetic fields were applied using the field-cooled (FC) magnetization protocol. As shown in the insets of Figure 2 and Figure S4 (Supporting Information), an abrupt rise in $\chi_m T$ and M at 20, 50, and 100 G occurred at 15 and 10 K for **1** and **2**, respectively, indicating the presence of weak ferromagnetism. The magnetic response was gradually suppressed with increasing external field. No appreciable peaks were observed in the ac susceptibility data (Figure S5, Supporting Information), suggesting that there is no long-range magnetic ordering in **1** and **2**. Thus, the apparent upturn in $\chi_m T$ supports the onset of spin canting in the antiferromagnetic homospin system. This characteristic feature is associated with operative single-ion anisotropy of the Mn(III) ion.[38,39] Such spin-canted behavior has also been observed in diverse coordination polymers involving Mn(III), Co(II), and Ni(II) spin centers connected by different bridging groups.[40−42]

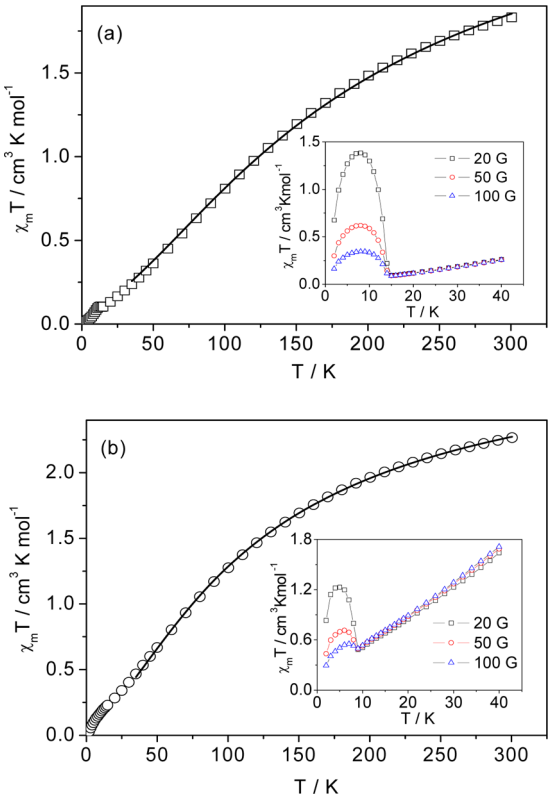

Figure 2. Plots of $\chi_m T$ versus *T* for (a) **1**·H_2O and (b) **2** at 1000 G. The solid lines in the main panel show the best magnetic fits. The insets denote the field-cooled magnetizations at the indicated external fields.

The intrachain magnetic exchange coupling constant was investigated by utilizing an infinite chain model ($H = -J\sum_i S_{Ai} \cdot S_{Ai+1}$) in the high-temperature regime to exclude the contributions from interchain magnetic interactions and zero-field splitting.[43] The best fit of the magnetic data to the Fisher equation produced the parameters $g = 2.01(1)$ and $J = -26.0(3)$ cm^{-1} for **1** at $T > 35$ K and $g = 2.029(3)$ and $J = -16.1(1)$ cm^{-1} for **2** at $T > 35$ K. Particularly, for compound **2**, there is a large disparity in Mn−N_3 bond lengths and angles for the three Mn centers. Therefore, the exchange parameter obtained for compound **2** is a mean value. The obtained coupling sign definitively confirms that antiferromagnetic exchange takes place between Mn spins within a chain and is transmitted via the EE azide linkage. Notably, the *J* value for **1** is a record high among EE azide-bridged Mn(III) systems.[22,23,27,28,32,33,36,37]

The field dependence of the magnetization was evaluated at 2 K in the field range of −7 to +7 T (Figures S6 and S7, Supporting Information). The magnetizations reached 0.11 μ_B for **1** and 0.58 μ_B for **2** at 7 T, which deviate significantly from that (4 μ_B) expected for the theoretical saturation value with $g = 2$. The low magnetization values are the result of the antiferromagnetic interactions between the Mn ions that lead to a nonmagnetic ground state at low temperature with a perturbation from spin canting. The linear magnetization region at high field was extrapolated to zero field to give 0.01 μ_B, and the canting angle, calculated as $\sin^{-1}(M_W/M_S)$, where M_S is the saturation magnetization and M_W is the magnetization induced by a weak magnetic field, was estimated to be 0.1° at 2 K for **1**. With use of the same procedure, the resulting mean canting angle of **2** was determined as 0.7°. The coercive field (H_{cr}) at 2 K was 800 G for **2**, while no H_{cr} was present for **1**. The disparity between H_{cr} of the two complexes likely originates from the different canting angles at 2 K.

Magnetostructural Correlation. The magnetic characters of several Mn(III) compounds bridged by EE azide groups are summarized on the basis of the pertinent internal parameters such as the Mn−$N(O)_{eq}$ and Mn−N_{ax} bond lengths and the Mn−N−N and Mn−N_{ax}···N_{ax}−Mn angles in the bridging routes (Table 1). The average Mn−$N(O)_{eq}$ lengths fall in the range 1.93−1.97 Å and are quite similar for the series. In the magnetic pathway, the average Mn−N_{ax} bond lengths deviate

dx.doi.org/10.1021/ic500676k | Inorg. Chem. 2014, 53, 7936−7940

Table 1. Specific Structural Parameters of Single EE Azide-Bridged Mn(III) Complexes and Their Magnetic Coupling Constants[a]

compd	av Mn−N(O)$_{eq}$ length (Å)	av Mn−N$_{ax}$ length (Å)	av Mn−N−N angle (deg)	av torsion angle (deg)	J (cm^{-1})[b]	ref
[Mn(salen)(N$_3$)]$_n$	1.93(6)	2.31(4)	117(3)	110(1)	−5.19(8)	37
[Mn(5-OCHH$_3$salen)(N$_3$)]$_n$	1.93(6)	2.324(3)	118(3)	105(1)	−6.00	28
[Mn(5-Brsalen)(N$_3$)]$_n$	1.93(6)	2.32(3)	119.3(4)	107(2)	−6.50	27
[Mn(3-MeOsalpn)(N$_3$)]·0.5NaClO$_4$	1.96(8)	2.23(1)	137(14)	118(3)	−6.54	23
[Mn(**L3**)(N$_3$)]$_n$	1.96(7)	2.29(5)	130(6)	116(3)	−7.3(1)	32
[Mn(**L4**)(N$_3$)]$_n$	1.93(8)	2.30(6)	116(8)	140(6)	−7.8(1)	33
[Mn(**L5**)(N$_3$)]$_n$	1.96(7)	2.28(1)	133(7)	126(4)	−8.0(1)	32
[Mn(salpn)(N$_3$)]$_n$	1.96(9)	2.34(1)	128(14)	127(1)	−8.06	36
[Mn(5-Fsalen)(N$_3$)]$_n$	1.93(6)	2.31(3)	117(3)	111(1)	−8.80	28
[Mn(3-MeOsalpn)(N$_3$)]·0.5RbClO$_4$	1.97(8)	2.29(1)	136(19)	104(9)	−9.73	23
[Mn(3-MeOsalpn)(N$_3$)]·0.5KClO$_4$	1.96(8)	2.23(2)	135(13)	116(4)	−9.84	23
[Mn(**L6**)(N$_3$)]$_n$	1.97(8)	2.26(3)	130(14)	146(19)	−11.5(1)	32
[Mn(**L2**)(N$_3$)] (**2**)	1.96(8)	2.27(4)	125(7)	151(6)	−16.1(1)	this work
[Mn(**L1**)(N$_3$)]·H$_2$O (**1**·H$_2$O)	1.93(8)	2.283(5)	121(1)	180	−26.0(3)	this work

[a]Abbreviations: salen = *N*,*N*′-ethylenebis(salicylideneiminate), 5-OCHH$_3$salen = *N*,*N*′-ethylenebis(5-methoxysalicylideneiminate), 5-Brsalen = *N*,*N*′-ethylenebis(5-bromosalicylideneiminate), 5-Fsalen = *N*,*N*′-ethylenebis(5-fluorosalicylideneiminate), 3-MeOsalpn = *N*,*N*′-(1,3-propylene)bis(3-methoxysalicylideneiminate), salpn = *N*,*N*′-(1,3-propylene)bis(salicylideneiminate), H$_2$**L1** = 2,2′-((1*E*,1′*E*)-ethane-1,2-diylbis(azan-1-yl-1-ylidene))-bis(phenylmethan-1-yl-1-ylidene)diphenol), H$_2$**L2** = 2,2′-((1*E*,1′*E*)-2,2-dimethylpropane-1,3-diyl)bis(azan-1-yl-1-ylidene)bis(phenylmethan-1-yl-1-ylidene)diphenol), H$_2$**L3**= *N*,*N*′-bis(5-chlorosalicylideneiminato)-1,3-diaminopentane, H$_2$**L4**= 2,2′-(((1*E*,1′*E*)-ethane-1,2-diylbis(azanylylidene))-bis(ethan-1-yl-1-ylidene))bis(4-chlorophenol), H$_2$**L5** = *N*,*N*′-bis(5-bromosalicylideneiminato)-1,3-diamino-2-dimethylpropane, H$_2$**L6** = *N*,*N*′-bis(5-bromosalicylideneiminato)-1,3-diaminopentane. [b]The 2*J* scheme in the exchange coupling Hamiltonian was converted to the *J* scheme for comparison.

slightly between 2.23 and 2.34 Å. The mean bridging angles of Mn−N−N vary from 117° to 136°. The bond length and angle variations are not reflective of the wide variation of the obtained coupling constants for the relevant complexes, although these parameters may affect magnetic coupling to some extent.[23,27,28,32,33,36,37] Although the aforementioned structural parameters vary minimally across the compounds, the average torsion angle (α) differs significantly. The plot of the J values as a function of α reveals that the absolute value of J is prone to increase as α becomes larger (Figure 3). By performing a linear fit of the data, the empirical formula of J (cm^{-1}) = 17.0° − 0.22α was roughly derived. The crossover point from antiferromagnetic to ferromagnetic interaction is estimated to be around 77°. The occurrence of the torsion angle below the predicted crossover angle could promote ferromagnetic coupling in the EE azide-bridged Mn(III) system as a consequence of the orthogonality of magnetic orbitals. In fact, intrachain ferromagnetic interactions were observed for EE azide-bridged Co(II), Ni(II), and Cu(II) chain systems in which the torsion angles were in the range 69.9−91.6°.[15,16,44] It should be noted that the J values for **1** and **2** are the record-high values for Mn(III) azide systems.[23,27,28,32,33,36,37] Thus, from the structural and magnetic considerations, deviation of the torsion angle from 90° allows for enhanced overlap of the magnetic orbitals and thus facilitates more effective antiferromagnetic interaction between the magnetic centers. In the simple orbital concept, the magnetic exchange in a Mn(III) system with a $t_{2g}^3e_g^1$ configuration can be interpreted by a combination of antiferromagnetic (J_{AF}) and ferromagnetic (J_F) contributions. The total coupling constant (J) equates to $J = (1/n_An_B)\sum_{ij}J_{ij} = J_{AF} + J_F$, where the J_{ij} values result from pairs of magnetic orbitals and n_A and n_B are the numbers of unpaired electrons.[45] In this scheme, J_{AF} is governed by the overlap integral between magnetic orbitals. Because **1** and **2** are one-dimensional chains with single EE azide bridges that bind to Mn(III) centers with long axial distances, the dominant exchange route is through the Mn d_{z^2} orbital. The relevant orbital will confer a σ-type pathway to the bridging azide involving the π orbitals.[28] The antiferromagnetic communication via the σ/π superexchange pathway will become stronger when the torsion angle increases from 90° to 180° due to the more effective overlaps between magnetic orbitals through the π-type ligand route, as observed in Figure 3. The J value (−26.0 cm^{-1}) for **1** is 2.3 times greater than the top J value (−11.5 cm^{-1}) of [Mn(**L5**)(N$_3$)]$_n$ (**L5**H$_2$ = *N*,*N*′-bis(5-bromosalicyli-

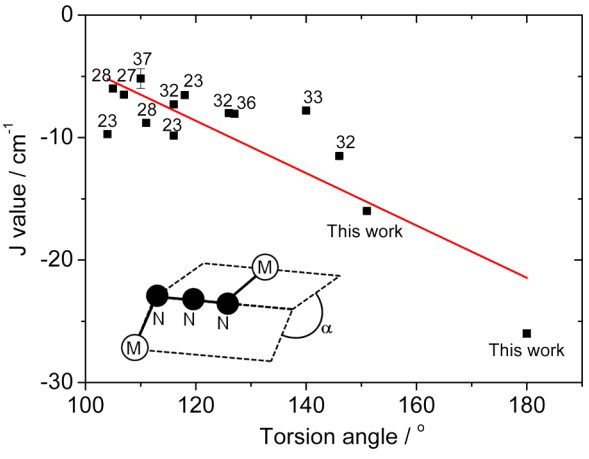

Figure 3. Relationship between the magnetic coupling constant (J) and the torsion angle Mn−N$_{ax}$···N$_{ax}$−Mn (α) for the EE azide-bridged Mn(III) systems. The inset shows a schematic illustration of the torsion angle. The numbers indicate the numbers of the references.

dx.doi.org/10.1021/ic500676k | Inorg. Chem. 2014, 53, 7936−7940

deneiminato)-1,3-diaminopentane) in the literature,[32] which is attributed to the largest torsion angle of 180° for **1**.

CONCLUSIONS

We have prepared two 1D Mn(III) coordination polymers bridged by azide in the EE mode, where the octahedral geometry around the Mn(III) ion undergoes Jahn−Teller distortion. A magnetostructural correlation based on the torsion angle in EE azide-bridged Mn(III) systems is established for the first time. Notably, the coupling constant (J) for **1** is a record high among EE azide-based Mn(III) systems, which is ascribed to the largest reported torsion angle of 180° in this chain. This work is the first demonstration of a direct structure−magnetic property relationship in azide-bridged Mn(III) systems.

ASSOCIATED CONTENT

Supporting Information

CIF files giving X-ray crystallographic data for complexes 1 and 2 and figures giving additional structural and magnetic data. This material is available free of charge via the Internet at http://pubs.acs.org.

AUTHOR INFORMATION

Corresponding Author

*E-mail for C.S.H.: cshong@korea.ac.kr.

Notes

The authors declare no competing financial interest.

ACKNOWLEDGMENTS

This work was supported by the Korea CCS R&D Center (KCRC) grant funded by the Korea government (The Ministry of Science, ICT & Future Planning (MSIP)) (NRF-2013M1A8A1035849), by the Basic Science Research Program (NRF-2012R1A1A2007141), and by the Priority Research Centers Program (NRF20100020209).

REFERENCES

(1) Wang, X.-Y.; Wang, Z.-M.; Gao, S. *Chem. Commun.* **2008**, 281−294.
(2) Escuer, A.; Vicente, R.; Goher, M. A. S.; Mautner, F. A. *Inorg. Chem.* **1996**, *35*, 6386−6391.
(3) Escuer, A.; Vicente, R.; Goher, M. A. S.; Mautner, F. A. *Inorg. Chem.* **1997**, *36*, 3440−3446.
(4) Escuer, A.; Cano, J.; Goher, M. A. S.; Journaux, Y.; Lloret, F.; Mautner, F. A.; Vicente, R. *Inorg. Chem.* **2000**, *39*, 4688−4695.
(5) Fu, A.; Huang, X.; Li, J.; Yuen, T.; Lin, C. L. *Chem. Eur. J.* **2002**, *8*, 2239−2247.
(6) Gao, E.-Q.; Wang, Z.-M.; Yan, C.-H. *Chem. Commun.* **2003**, 1748−1749.
(7) Escuer, A.; Mautner, F. A.; Goher, M. A.; Abu-Youssef, M. A.; Vicente, R. *Chem. Commun.* **2005**, 605−607.
(8) Liu, X. T.; Wang, X. Y.; Zhang, W. X.; Cui, P.; Gao, S. *Adv. Mater.* **2006**, *18*, 2852−2856.
(9) Wang, X.-Y.; Wang, L.; Wang, Z.-M.; Gao, S. *J. Am. Chem. Soc.* **2006**, *128*, 674−675.
(10) Li, R.-Y.; Wang, X.-Y.; Liu, T.; Xu, H.-B.; Zhao, F.; Wang, Z.-M.; Gao, S. *Inorg. Chem.* **2008**, *47*, 8134−8142.
(11) Li, R.-Y.; Wang, Z.-M.; Gao, S. *CrystEngComm* **2009**, *11*, 2096−2101.
(12) Ma, Y.; Zhang, J. Y.; Cheng, A. L.; Sun, Q.; Gao, E. Q.; Liu, C. M. *Inorg. Chem.* **2009**, *48*, 6142−6151.
(13) Adhikary, C.; Koner, S. *Coord. Chem. Rev.* **2010**, *254*, 2933−2958.
(14) Hong, C. S.; Do, Y. *Angew. Chem., Int. Ed.* **1999**, *38*, 193−195.
(15) Hong, C. S.; Koo, J.-e.; Son, S.-K.; Lee, Y. S.; Kim, Y.-S.; Do, Y. *Chem. Eur. J.* **2001**, *7*, 4243−4252.
(16) Yoo, H. S.; Kim, J. I.; Yang, N.; Koh, E. K.; Park, J.-G.; Hong, C. S. *Inorg. Chem.* **2007**, *46*, 9054−9056.
(17) Liu, T.-F.; Fu, D.; Gao, S.; Zhang, Y.-Z.; Sun, H.-L.; Su, G.; Liu, Y.-J. *J. Am. Chem. Soc.* **2003**, *125*, 13976−13977.
(18) Yin, P.; Gao, S.; Zheng, L.-M.; Wang, Z.; Xin, X.-Q. *Chem. Commun.* **2003**, 1076−1077.
(19) Gao, E. Q.; Liu, P. P.; Wang, Y. Q.; Yue, Q.; Wang, Q. L. *Chem. Eur. J.* **2009**, *15*, 1217−1226.
(20) Jia, Q.-X.; Tian, H.; Zhang, J.-Y.; Gao, E.-Q. *Chem. Eur. J.* **2011**, *17*, 1040−1051.
(21) Weng, D.-F.; Wang, Z.-M.; Gao, S. *Chem. Soc. Rev.* **2011**, *40*, 3157−3181.
(22) Miyasaka, H.; Saitoh, A.; Abe, S. *Coord. Chem. Rev.* **2007**, *251*, 2622−2664.
(23) Yoon, J. H.; Lee, J. W.; Ryu, D. W.; Yoon, S. W.; Suh, B. J.; Kim, H. C.; Hong, C. S. *Chem. Eur. J.* **2011**, *17*, 3028−3034.
(24) Yoon, J. H.; Ryu, D. W.; Kim, H. C.; Yoon, S. W.; Suh, B. J.; Hong, C. S. *Chem. Eur. J.* **2009**, *15*, 3661−3665.
(25) Saha, S.; Mal, D.; Koner, S.; Bhattacherjee, A.; Gütlich, P.; Mondal, S.; Mukherjee, M.; Okamoto, K.-I. *Polyhedron* **2004**, *23*, 1811−1817.
(26) Ge, C.-H.; Cui, A.-L.; Ni, Z.-H.; Jiang, Y.-B.; Zhang, L.-F.; Ribas, J.; Kou, H.-Z. *Inorg. Chem.* **2006**, *45*, 4883−4885.
(27) Ko, H. H.; Lim, J. H.; Kim, H. C.; Hong, C. S. *Inorg. Chem.* **2006**, *45*, 8847−8849.
(28) Yuan, M.; Zhao, F.; Zhang, W.; Wang, Z.-M.; Gao, S. *Inorg. Chem.* **2007**, *46*, 11235−11242.
(29) Viciano-Chumillas, M.; Tanase, S.; Mutikainen, I.; Turpeinen, U.; de Jongh, L. J.; Reedijk, J. *Inorg. Chem.* **2008**, *47*, 5919−5929.
(30) Liu, C. M.; Zhang, D. Q.; Zhu, D. B. *Inorg. Chem.* **2009**, *48*, 4980−4987.
(31) Stamatatos, T. C.; Christou, G. *Inorg. Chem.* **2009**, *48*, 3308−3322.
(32) Yoon, J. H.; Lee, W. R.; Ryu, D. W.; Lee, J. W.; Yoon, S. W.; Suh, B. J.; Kim, H. C.; Hong, C. S. *Inorg. Chem.* **2011**, *50*, 10777−10785.
(33) Chakrabarty, P. P.; Saha, S.; Schollmeyer, D.; Boudalis, A. K.; Jana, A. D.; Luneau, D. *J. Coord. Chem.* **2013**, *66*, 9−17.
(34) McInnes, J. M.; Swallow, D.; Blake, A. J.; Mountford, P. *Inorg. Chem.* **1998**, *37*, 5970−5977.
(35) Corden, J. P.; Errington, W.; Moore, P.; Phillips, P. R.; Wallbridge, M. G. H. *Acta Crystallogr., Sect. C* **1996**, *C52*, 3199−3202.
(36) Reddy, K. R.; Rajasekharan, M. V.; Tuchagues, J.-P. *Inorg. Chem.* **1998**, *37*, 5978−5982.
(37) Panja, A.; Shaikh, N.; Vojtíšek, P.; Gao, S.; Banerjee, P. *New J. Chem.* **2002**, *26*, 1025−1028.
(38) Dzyaloshinsky, L. *J. Phys. Chem. Solids* **1958**, *4*, 241−255.
(39) moriya, T. *Phys. Rev.* **1960**, *120*, 91−98.
(40) Bellitto, C.; Bauer, E. M.; Ibrahim, S. A.; Mahmoud, M. R.; Righini, G. *Chem. Eur. J.* **2003**, *9*, 1324−1331.
(41) Abu-Youssef, M. A. M.; Mautner, F. A.; Vicente, R. *Inorg. Chem.* **2007**, *46*, 4654−4659.
(42) Cao, D.-K.; Li, Y.-Z.; Zheng, L.-M. *Inorg. Chem.* **2007**, *46*, 7571−7578.
(43) Fisher, M. E. *Am. J. Phys.* **1964**, *32*, 343−346.
(44) Maji, T. K.; Mukherjee, P. S.; Mostafa, G.; Mallah, T.; Cano-Boquera, J.; Chaudhuri, N. R. *Chem. Commun.* **2001**, 1012−1013.
(45) Kahn, O. *Molecular Magnetism*; VCH: New York, 1993.